X-ray constraints on dark photon tridents

Tim Linden,[1,*] Thong T. Q. Nguyen,[1,†] and Tim M. P. Tait[2,‡]
[1]*Stockholm University and The Oskar Klein Centre for Cosmoparticle Physics, Alba Nova, 10691 Stockholm, Sweden*
[2]*Department of Physics and Astronomy, University of California, Irvine, California 92697 USA*

(Received 25 July 2024; accepted 16 June 2025; published 17 July 2025)

Dark photons that are sufficiently light and/or weakly interacting represent a compelling vision of dark matter. Dark photon decay into three photons, which we call the dark photon trident, can be the dominant channel when the dark photon mass falls below the electron pair threshold and can produce a significant flux of x rays. We use 16 years of data from Interrnational Gamma-Ray Astro Physics Laboratory (INTEGRAL)/Spectrometer of INTEGRAL (SPI) to constrain sub-MeV dark photon decay, producing new worlds-best constraints on the kinetic mixing parameter for dark photon masses between 90 and 1022 keV, and comment on the potential for future x-ray observatories to discover the trident decay process.

DOI: 10.1103/37gn-x3y1

I. INTRODUCTION

The dark photon is a hypothetical massive spin-1 particle that exists in many extensions of the Standard Model (SM) incorporating an extra $U(1)$ gauge symmetry whose corresponding gauge boson interacts with the SM fermions via kinetic mixing with the SM photon [1–7]. It is typically categorized as a weakly interacting slim particle [8]. Dark photons are the target of a rich array of both high-energy and astrophysical searches for beyond Standard Model particles [9–26].

Provided its mass and kinetic mixing are chosen such that it is stable on cosmological time scales, a dark photon can play the role of the dark matter [7,10,27–30]. However, nonzero kinetic mixing implies that dark photons eventually decay into potentially observable SM particles. For a given mass, the end products of decay are determined by the kinematically accessible SM particles. The subsequent interactions of these particles can produce a distribution of bright photon signals that can be detected across the electromagnetic spectrum.

The situation is much simpler, however, if the dark photon mass falls below twice the electron mass. In this case, only photon and neutrino final states are kinematically accessible. Since the two-photon final state is forbidden by the Landau-Yang theorem [31,32] and decays to neutrinos are highly suppressed, the dominant channel is the three-photon final state through a process which we term the "dark photon trident." Decays into photon tridents produce a unique spectrum that is broader than the line spectrum from two-photon states [33]. While a combination of astrophysical and direct-detection constraints rule out large kinetic couplings through much of the sub-MeV mass range [8], there are notable sensitivity gaps in the x-ray band.

The primary difficulty in constraining dark photon decays stems from the extremely diffuse morphology of the resulting x-ray signal. For standard Navarro-Frenk-White (NFW) profiles, the most sensitive decay searches are those which observe as much of the sky as possible. This makes investigations with high-resolution telescopes such as Chandra or XMM-Newton difficult. However, wide-field-of-view telescopes, such as Interrnational Gamma-Ray Astro Physics Laboratory (INTEGRAL), are highly effective for dark matter decay searches.

In this paper, we use 16 years of x-ray data from INTEGRAL/Spectrometer of INTEGRAL (SPI) to strongly constrain dark matter decays via photon tridents in the regime where the dark photon mass is below twice the electron mass. Figure 1 shows our result, which improves current constraints on the dark photon lifetime by more than an order of magnitude between 61 and 1022 keV. Compared to previous work, our limits are significantly strengthened by the inclusion of the full one-loop amplitude for the dark photon decay, in contrast to the leading Euler-Heisenberg approximation used in previous analyses [9,10]. Our results strongly motivate further dark photon searches with next-generation x-ray telescopes.

*Contact author: linden@fysik.su.se
†Contact author: thong.nguyen@fysik.su.se
‡Contact author: ttait@uci.edu

Published by the American Physical Society under the terms of the Creative Commons Attribution 4.0 International license. Further distribution of this work must maintain attribution to the author(s) and the published article's title, journal citation, and DOI. Funded by SCOAP³.

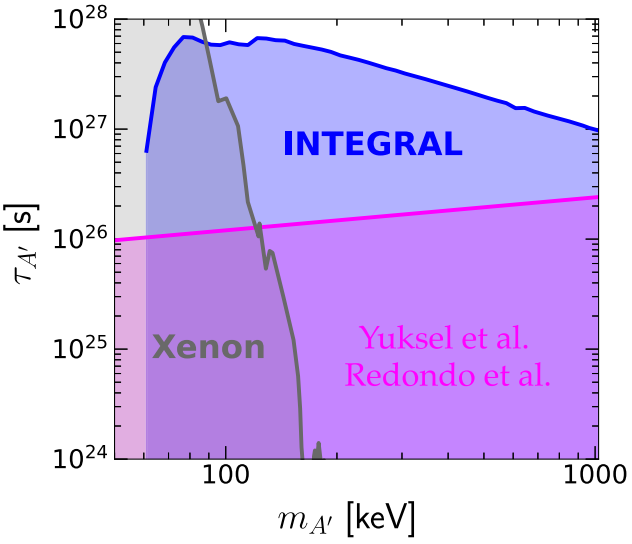


FIG. 1. 95% C.L. INTEGRAL upper limits (blue line) on the dark photon dark matter lifetime based on the three photon decay channel. Previous constraints based on the diffuse x-ray background in magenta from Ref. [38] (model independent) and from Refs. [9,10] are shown for the same dark photon trident. Direct detection constraints from Xenon are shown in gray [11–15].

II. DARK PHOTON TRIDENT

The Lagrangian describing a massive dark photon $m_{A'}$ and its interactions with SM particles is given by

$$\mathcal{L} \supset -\frac{1}{4}F'_{\mu\nu}F'^{\mu\nu} - \frac{1}{2}m_{A'}^2 A'_\mu A'^\mu - \frac{\epsilon}{2}F'_{\mu\nu}F^{\mu\nu}, \tag{1}$$

where the field strength tensors are $F'_{\mu\nu} = \partial_\mu A'_\nu - \partial_\nu A'_\mu$, etc. For nonzero values of ϵ, the dark photon kinetically mixes with the SM photon, allowing it to decay into any SM particles that also interact with the photon.

For dark photon masses below twice the electron mass, the dominant decay channels include three-photon final states, which we show in Fig. 2 and call the dark photon trident. The only other kinematically allowed final states are SM neutrinos, which result from mixing between the dark photon and the SM Z boson (see Refs. [34–36] for discussion of the indirect searches). However, these are strongly suppressed by the large Z mass and are ignored throughout the remainder of this work. Previous work [6,9] computed the photon trident rate using the leading dimension-8 term in an effective field theory (EFT) obtained (for $m_A \ll 2m_e$) by integrating out heavy SM fermion fields at one loop (see Fig. 2),

$$\mathcal{L}^{\rm EH}_{A'} = \frac{\epsilon\alpha_{\rm em}}{45m_e^4}(14F'_{\mu\nu}F^{\nu\lambda}F_{\lambda\rho}F^{\rho\mu} - 5F'_{\mu\nu}F^{\mu\nu}F_{\alpha\beta}F^{\alpha\beta}), \tag{2}$$

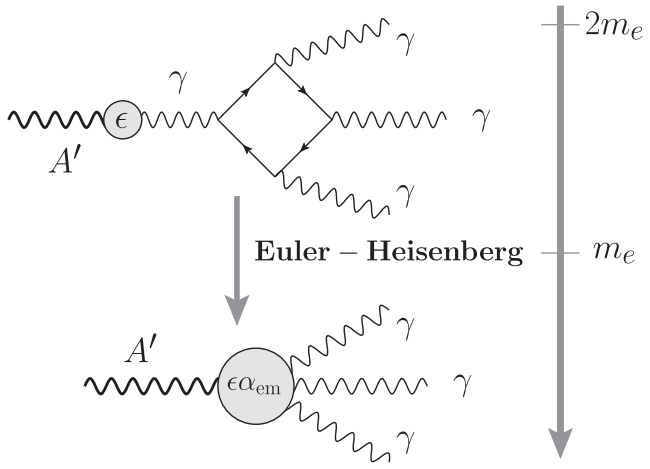


FIG. 2. Schematic illustration showing how the Euler-Heisenberg effective field theory (bottom) results from integrating out loops of SM charged fermions (top) in the limit $m_A \ll 2m_e$.

which results in an expression for the decay width in the leading EFT Euler-Heisenberg (EH) limit [33]:

$$\Gamma_{\rm EH} = \frac{17\epsilon^2\alpha_{\rm em}^4}{11664000\pi^3} \times \frac{m_{A'}^9}{m_e^8} \simeq 1{\rm s}^{-1} \times \left(\frac{\epsilon}{0.003}\right)^2 \times \left(\frac{m_{A'}}{m_e}\right)^9. \tag{3}$$

However, the leading EFT approximation breaks down for $m_{A'} \sim m_e$. The full decay width can be related to the Euler-Heisenberg approximation [37],

$$\Gamma_{A'\to 3\gamma} = \Gamma_{\rm EH} \times f_{\rm loop}(m_{A'}), \tag{4}$$

where $f_{\rm loop}(m_{A'})$ is an enhancement factor that depends on the dark photon mass, computed in Ref. [37].

Throughout this work, we assume the dark photon makes up the entirety of the dark matter in the Universe. It can be produced via the misalignment mechanism and/or nonthermal production during inflation, when the DM mass arises through the Stüeckeblberg mechanism [7,10]. The photon flux from dark photon decays is

$$\frac{{\rm d}\Phi_\gamma}{{\rm d}E_\gamma} = \frac{\Gamma}{4\pi m_{\rm DM}} \times \frac{{\rm d}N_\gamma}{{\rm d}E_\gamma} \times D, \tag{5}$$

where $\Gamma \equiv \Gamma_{A'\to 3\gamma}$ and $m_{\rm DM} \equiv m_{A'}$. The energy spectrum for dark photon trident decay is given by [33,39]

$$\frac{{\rm d}N_\gamma}{{\rm d}E_\gamma} = \frac{2x^3}{17m_{A'}}\left(1715 - 3105x + \frac{2919}{2}x^2\right), \tag{6}$$

where $x = 2E_\gamma/m_{A'}$ runs between 0 and 1. The D factor in Eq. (5) depends on the dark matter density profile of the Milky Way, integrated over the line of sight s,

$$D = \int d\Omega \int ds \rho(r(s,l,b)). \quad (7)$$

where l and b are Galactic longitude and latitude and the differential solid angle $d\Omega = \cos l dl db$. We assume a NFW dark matter density profile with $r_s = 9.98$ kpc and $\rho_\odot = 0.42$ GeV/cm^3 [40]. For the region of interest (ROI) in the Galactic halo with longitude $|l| \leq 47.5°$ and latitude $|b| \leq 47.5°$, we obtain $D = 1.3 \times 10^{23}$ GeV/cm^2 [41].

However, INTEGRAL data analysis requires the removal of a isotropic emission sources, which are dominated by cosmic-ray contamination. Thus, we remove the isotropic portion of the dark matter annihilation signal setting the D factor over the most distant region of our ROI (47.5°) to 0 and renormalize the remaining dark matter signal. This leaves us with an effective D factor of $D = 1.2 \times 10^{23}$ GeV/cm^2, which we use for our analysis. We note that this choice also effectively removes any isotropic x-ray background from extragalactic sources from our analysis [42].

We do not consider dark photon masses above $2m_e$. Despite the fact that such heavier dark photons can produce a significant photon flux from final-state radiation [43], this region is already stringently constrained by beam dump experiments [44] and model-dependent constraints from the cosmic microwave background [45] and big bang nucleosynthesis [46–48].

III. INTEGRAL/SPI ANAYLYSIS

INTEGRAL is a hard x-ray space telescope. Using the SPI, it uniquely probes an important energy range that lies between 30 and 8 MeV. INTEGRAL observations open many opportunities in the field of astrophysics [49–54] as well as searches for novel phenomena [42,55–59].

Following the framework of previous studies focused on decays of axions and sterile neutrinos [55], as well as primordial black holes [57], we study the dark photon trident with 16 years of INTEGRAL/SPI data. Since we are interested in photons with energies below 511 keV, the diffuse background model we consider in this study contains three main components [60], which are shown in Fig. 3:

(i) unresolved point sources (red bands) described by a power-law with an exponential cutoff [61],
(ii) inverse Compton scattering of interstellar radiation fields described by a power-law spectrum (green bands) [62],
(iii) emission produced by positronium decays are in (cyan bands) with a normalization that is strongly constrained by 511 keV line observations [50].

Additionally, there is a nuclear line at 478 keV from ^{7}Be, but its contribution is negligible [63]. Analytic spectra for these components are shown in the Appendix. The total diffuse flux is the combination of these components, shown at 1σ and 2σ in the purple bands. Figure 3 also depicts a

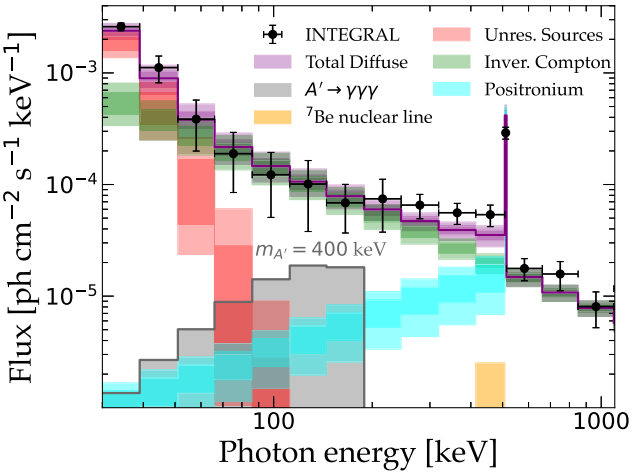


FIG. 3. The INTEGRAL photon flux and models for different sources. The observed data between 30–1022 keV are shown as black points. The best fit, along with 1σ and 2σ error bands for the astrophysical source classes, are depicted as follows: red for unresolved sources, green for inverse Compton scattering, cyan for positronium decay with an intensity fit to the 511 keV line, and orange for the ^{7}Be nuclear line. The total diffuse flux that fits the data is in purple. For comparison, we also show an arbitrarily normalized spectrum for the dark photon trident from a 400 keV dark photon (gray band), which is not included in the fit.

2-sigma uncertainty band for 400 keV dark photon decays as the gray band, which has a peak around $m_{A'}/3$, with the spectral shape from Eq. (6). The normalization of this component is arbitrary and not included in the total diffuse fit.

We consider photon energies between 30–511 keV. We set a 95% C.L. upper limit on the dark matter decay timescale by fitting the dark matter component along with the arbitrary normalizations of each astrophysical component to INTEGRAL/SPI data. Using the 3 ML package [64] with the EMCEE Markov chain Monte Carlo method [65], we sample all free spectral parameters, including the decay width of the dark photon trident. We utilize prior distributions that prevent unphysical results (e.g., negative fluxes from any source class). The template and codes used in our analysis are publicly available and stem from previous work on dark matter decays in Refs. [55,57], published on the Zenodo repository.

IV. CONSTRAINTS ON DARK PHOTON DARK MATTER

In Fig. 1 (blue), we show the 95% C.L. upper limits on the dark matter lifetime in the case of dark photon trident decay using 16 years of INTEGRAL/SPI data. We compare our result with two existing constraints: dark photon direct detection results from Xenon in gray [13] and previous searches for the same dark photon trident from Refs. [9,38] in magenta. Our constraint also applies to other spin-1 dark matter models with a ∼100% branching ratio into the three photons final states.

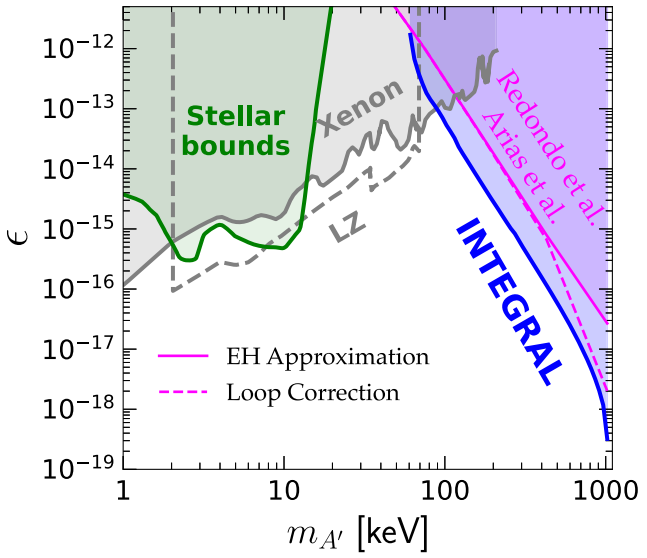


FIG. 4. New constraints on the plane of the kinetic mixing and the dark photon mass using INTEGRAL/SPI are shown in blue. Previous constraints based on this decay process based on the diffuse x-ray background is in magenta: the solid line is the leading EFT result [8–10], and the dashed line includes the full one-loop decay amplitude. Constraints on dark photon from direct searches are shown in gray: the solid line is from Xenon, and the dashed line is the projection for LZ [11–15]. The combined constraints from studies of dark photon production in stars (stellar bounds) are in green and follow the results of Refs. [16–18,20–26].

We map the constraints on the dark photon lifetime into constraints on the maximum allowed kinetic mixing parameter (using the one-loop decay amplitude). These constraints are shown as the blue line in Fig. 4. Direct detection constraints from Xenon and projections for Lux-Zepplin (LZ) [11–14] are indicated by the solid and dashed gray lines. The constraints from the dark photon trident using the intergalactic diffuse background limit (in the Euler-Heisenberg approximation) from Refs. [9,10] are the solid magenta line. The constraint that they would have obtained from the one-loop amplitude is shown as the dashed magenta line.

We also include the combined constraints from numerous studies of dark photon production in stellar environments as the green line, which can reach comparable strengths as LZ at low dark photon masses [16–18,20–26]. We do note that, unlike the other constraints in this paper, stellar bound constraints have the advantage that they do not assume that the dark photon composes all (or even any) of the dark matter. However, their range is limited by the small plasma temperature of stellar objects, which limits the ability for stars to produce dark photons with masses above a few tens of keV [66]. Thus, our study demonstrates the unique power of diffuse x-ray data to probe a unique dark matter mass range where other techniques are insensitive.

We finally compare our results with previous diffuse x-ray searches for dark photon trident decays from Refs. [9,10]. We note that our constraints significantly exceed previous work, even though both studies also used SPI [67] data (in addition to COMPTEL [68] and EGRET [69] data) in their analysis. The strength of our constraints can be explained by three factors, which are listed in order of decreasing importance:

(i) We take into account astrophysical background contributions, while Refs. [9,10] used the benchmark from Ref. [38], which conservatively assumed that the observed photon signal is entirely produced by dark matter.
(ii) We use the full one-loop calculation, instead of the leading EFT approximation used in Ref. [9].
(iii) We use 16 years of data calibration, while Ref. [38] used only 6 years of SPI observation.

The improved background modeling is the primary effect and itself improves our constraint by around 1 order of magnitude, compared to Refs. [9,10], even if the full one-loop decay amplitude were to be employed in both studies. This not only places new constraints on the dark photon dark matter model but also again demonstrates the important of understanding astrophysical backgrounds for dark matter searches.

Note that in this study we only examine dark photon masses below the electron-positron pair threshold. For larger masses, the dominant decay channel is into electron-positron pairs that can subsequently radiate photons via final-state radiation. The energy of such photons can populate the INTEGRAL search range, and thus it may be possible to set limits on dark photons with higher masses using this analysis. Since the motivation of this paper is to focus on the dark photon trident process, we leave investigation of this possibility for future work [70–72].

V. CONCLUSION AND OUTLOOK

In this paper, we study the decay of dark photon dark matter using 16 years of INTEGRAL/SPI data in the mass range of 60–1022 keV. Concentrating on the case where the three photon final state (dark photon trident) is the dominant decay channel, we provide new constraints on kinetic mixing and dark photon mass that exceed previous results by nearly 2 orders of magnitude. Taking into account astrophysical background and the full one-loop decay amplitude, we constrain the kinetic mixing coupling from 10^{-12} down to 10^{-19} in the 61–1022 keV mass range of dark photon.

This study also motivates other searches for dark photon tridents. Since the dark photon is a weakly interacting slim particle and has similar decay signal as the axion and axionlike-particles, many studies and techniques for weakly interacting slim particle searches can also be applied to the dark photon [73]. Our results motivate exploring existing x-ray and IR searches for axions, to

see how they apply to the dark photon trident process, such as, for example, Chandra [74–77]; XMM-Newton [78,79]; NuSTAR [80–82]; eROSITA [83]; JWST [84–88]; MUSE [89]; and future observations such as THESEUS [90], ASTROMEV [91], XRISM [92], Athena [93,94], Axis [94], and EuXFEL [95].

This work made use of NUMPY [96], SCIPY [97], ASTROPY [98], MATPLOTLIB [99], JUPYTER [100], JAXODRAW [101], and WEBPLOTDIGITIZER [102].

ACKNOWLEDGMENTS

We especially thank Francesca Calore and Thomas Siegert for sharing the modeling code from Ref. [55], which were used in this analysis. We also grateful for Ciaran O'Hare's comments on other existing constraints from his website. We thank Carlos Blanco, Christopher Dessert, Ludvig Doeser, Júlia Sisk-Reynés, Nick Rodd, and Axel Widmark for fruitful discussions. T. L. and T. T. Q. N. acknowledge support by the Swedish Research Council under Contract No. 2022-04283. T. T. Q. N. is also grateful for the supported by the COST Action COSMIC WISPers Grant No. CA21106, supported by COST (European Cooperation in Science and Technology), and thanks the Galileo Galilei Institute for Theoretical Physics for the hospitality and the INFN for partial support during the completion of this work. T. M. P. T. is supported by the US National Science Foundation under Grant No. PHY-2210283.

APPENDIX A: DARK PHOTON TRIDENT DECAY WIDTH AND ENERGY SPECTRUM

We consider a dark photon decay into three photons through a loop induced by a fermion in Fig. 2, with the most significant contribution coming from the electron. The resulting amplitude can be parametrized as

$$\begin{aligned} i\mathcal{M} &\equiv i\mathcal{M}(p,k_1,k_2,k_3,h,s_1,s_2,s_3) \\ &= i\mathcal{A}^{\mu\nu\rho\sigma}\epsilon(p,h)\epsilon^*(k_1,s_1)\epsilon^*(k_2,s_2)\epsilon^*(k_3,s_3), \end{aligned} \tag{A1}$$

where (p, h) and (k_i, s_i) are the momenta and polarizations of the initial dark photon and each final ith photon. For loop momentum q, the contribution from a single fermion to $\mathcal{A}^{\mu\nu\rho\sigma}$ is

$$\begin{aligned} i\mathcal{A}^{\mu\nu\rho\sigma} = 2\epsilon e^4\Bigg[&\int\frac{\mathrm{d}^4q}{(2\pi)^4}\frac{\mathrm{Tr}[\gamma^\mu(\not{q}+m_e)\gamma^\nu(\not{q}+\not{k}_1+m_e)\gamma^\rho(\not{q}+\not{k}_1+\not{k}_2+m_e)\gamma^\sigma(\not{q}+\not{p}+m_e)]}{(q^2+m_e^2)[(q+k_1)^2+m_e^2][(q+k_1+k_2)^2+m_e^2][(q+p)^2-m_e^2]} \\ &+\int\frac{\mathrm{d}^4q}{(2\pi)^4}\frac{\mathrm{Tr}[\gamma^\mu(\not{q}+m_e)\gamma^\rho(\not{q}+\not{k}_2+m_e)\gamma^\nu(\not{q}+\not{k}_1+\not{k}_2+m_e)\gamma^\sigma(\not{q}+\not{p}+m_e)]}{(q^2+m_e^2)[(q+k_2)^2+m_e^2][(q+k_1+k_2)^2+m_e^2][(q+p)^2-m_e^2]} \\ &+\int\frac{\mathrm{d}^4q}{(2\pi)^4}\frac{\mathrm{Tr}[\gamma^\mu(\not{q}+m_e)\gamma^\nu(\not{q}+\not{k}_1+m_e)\gamma^\sigma(\not{q}+\not{p}-\not{k}_2+m_e)\gamma^\rho(\not{q}+\not{p}+m_e)]}{(q^2+m_e^2)[(q+k_1)^2+m_e^2][(q+p-k_2)^2+m_e^2][(q+p)^2-m_e^2]}\Bigg], \end{aligned} \tag{A2}$$

where m_e is the mass of the fermion. The squared amplitude, summed over all final-state polarizations and averaged over the initial three polarizations of massive dark photon, is

$$\overline{|\mathcal{M}|^2} = \frac{1}{3}\mathcal{A}^{\mu\nu\rho\sigma}(\mathcal{A}^*)^{\dot\mu\dot\nu\dot\rho\dot\sigma}\left(-g_{\mu\dot\mu}+\frac{p_\mu p_{\dot\mu}}{m_{A'}^2}\right)(-g_{\nu\dot\nu})(-g_{\rho\dot\rho})(-g_{\sigma\dot\sigma}) = \frac{1}{3}\mathcal{A}^{\mu\nu\rho\sigma}(\mathcal{A}^*)_{\mu\nu\rho\sigma}. \tag{A3}$$

The dark photon trident decay width at one loop is

$$\Gamma_{A'\to3\gamma} = \frac{1}{(2\pi)^3}\frac{1}{32m_{A'}^2}\frac{1}{6}\int_0^{m_{A'}^2}\mathrm{d}m_{12}^2\int_0^{m_{A'}^2-m_{12}^2}\mathrm{d}m_{13}^2\times\overline{|\mathcal{M}|^2}, \tag{A4}$$

with kinematic variables $m_{ij}^2=(k_i+k_j)^2$, and the factor $1/6$ is for three identical particles in the final state. Comparing this result to the Euler-Heisenberg approximation in Eq. (3), this decay width can be parametrized following Ref. [37]:

$$\Gamma_{A'\to3\gamma} = \Gamma_{\mathrm{EH}}\times f_{\mathrm{loop}}(m_{A'}) = \Gamma_{\mathrm{EH}}\left[1+\sum_{n=1}^{\infty}c_k\left(\frac{m_{A'}^2}{m_e^2}\right)^n\right], \tag{A5}$$

where the coefficients c_n which encode the ratio between the full one-loop and leading EFT approximation are calculated in Ref. [37].

The energy spectrum in Eq. (5) is proportional to the decay width differential in the energy of one photon [33],

$$\begin{aligned} \frac{1}{N}\frac{\mathrm{d}N}{\mathrm{d}x} &= \frac{1}{\Gamma_{A'\to3\gamma}}\frac{\mathrm{d}\Gamma_{A'\to3\gamma}}{\mathrm{d}x} = \frac{1}{\Gamma_{\mathrm{EH}}}\frac{\mathrm{d}\Gamma_{\mathrm{EH}}}{\mathrm{d}x} \\ &= \frac{1}{51}x^3\left(1715-3105x+\frac{2919}{2}x^2\right), \end{aligned} \tag{A6}$$

where $x=2E_\gamma/m_{A'}$. Notably, the energy spectrum is independent of the dark photon mass.

APPENDIX B: DIFFUSE ASTROPHYSICAL BACKGROUND

To model the astrophysical background, we consider three main components that produce diffuse photons below 1 MeV:

(i) The first component arises from unresolved sources and is modeled as a power-law spectrum with an exponential cutoff,

$$\Phi_{\rm unres} = C_0 \left(\frac{E}{E_0}\right)^{\alpha_0} \exp\left(-\frac{E}{E_C}\right). \quad \text{(B1)}$$

(ii) The second component is due to inverse-Compton scattering, which follows a power-law spectrum,

$$\Phi_{\rm IC} = C_1 \left(\frac{E}{E_1}\right)^{\alpha_1}. \quad \text{(B2)}$$

(iii) The third component is the positronium decay spectrum, with an amplitude fit to the 511 keV line flux, $\Phi_{\rm posi} = F(E, f_{\rm Ps}, F_{511})$, that is described in Ref. [51].

(iv) The fourth component comes from nuclear line emission, with the dominant contribution from ^{7}Be. This is modeled by a Gaussian:

$$\Phi_{\rm Be} = \frac{F_{\rm Be}}{\sqrt{2\pi}\sigma_{\rm Be}} \exp\left(-\frac{(E-\mu_{\rm Be})^2}{2\sigma_{\rm Be}^2}\right), \quad \text{(B3)}$$

where the Gaussian width corresponds primarily to the instrumental energy resolution.

These spectra are imported from the 3 ML package [64]. All parameters' values and prior distributions are listed in Table I.

TABLE I. Parameter values, scan ranges, and their prior distributions in our EMCEE Markov chain Monte Carlo sampling priors for the astrophysical background, encoded in the 3 ML package. See also Ref. [58].

Sources (spectrum)	Parameter	Fix/free	Value/range	Unit	Prior distribution
Unresolved sources	C_0	Free	10^{-5}–1.0	keV^{-1} s^{-1} cm^{-2}	Log uniform
	E_0	Fix	50	keV	⋯
	α_0	Fix	0.0	⋯	⋯
	E_C	Free	1–100	keV	Truncated Gaussian
Inverse Compton	C_1	Free	10^{-10}–1.0	keV^{-1} s^{-1} cm^{-2}	Log uniform
	E_1	Fix	1000	keV	⋯
	α_1	Free	−3.0–0.0	⋯	Uniform
Positronium	F_{511}	Free	10^{-6}–0.1	s^{-1} cm^{-2}	Log uniform
	$f_{\rm Ps}$	Free	0.0–1.0	⋯	Truncated Gaussian
Nuclear line (^{7}Be)	$F_{\rm Be}$	Free	10^{-10}–1.0	s^{-1} cm^{-2}	Log uniform
	$\sigma_{\rm Be}$	Fix	2.4	keV	⋯
	$\mu_{\rm Be}$	Fix	478	keV	⋯

[1] B. Holdom, Phys. Lett. **166B**, 196 (1986).
[2] P. Fayet, Phys. Lett. **95B**, 285 (1980).
[3] P. Fayet, Nucl. Phys. **B347**, 743 (1990).
[4] M. Fabbrichesi, E. Gabrielli, and G. Lanfranchi, *The Physics of the Dark Photon* (Springer, Cham, 2021).
[5] T. G. Rizzo, J. High Energy Phys. 07 (2018) 118.
[6] M. Pospelov, Phys. Rev. D **80**, 095002 (2009).
[7] A. E. Nelson and J. Scholtz, Phys. Rev. D **84**, 103501 (2011).
[8] A. Caputo, C. A. J. O'Hare, A. J. Millar, and E. Vitagliano, Phys. Rev. D **104**, 095029 (2021).
[9] J. Redondo and M. Postma, J. Cosmol. Astropart. Phys. 02 (2009) 005.
[10] P. Arias, D. Cadamuro, M. Goodsell, J. Jaeckel, J. Redondo, and A. Ringwald, J. Cosmol. Astropart. Phys. 06 (2012) 013.
[11] I. M. Bloch, R. Essig, K. Tobioka, T. Volansky, and T.-T. Yu, J. High Energy Phys. 06 (2017) 087.
[12] E. Aprile *et al.* (XENON Collaboration), Phys. Rev. Lett. **123**, 251801 (2019).
[13] E. Aprile *et al.* (XENON Collaboration), Phys. Rev. D **102**, 072004 (2020).

[14] E. Aprile *et al.* (XENON Collaboration), Phys. Rev. D **106**, 022001 (2022).
[15] H. An, M. Pospelov, J. Pradler, and A. Ritz, Phys. Rev. D **102**, 115022 (2020).
[16] E. Fischbach, H. Kloor, R. A. Langel, A. T. Y. Liu, and M. Peredo, Phys. Rev. Lett. **73**, 514 (1994).
[17] H.-S. Zechlin, D. Horns, and J. Redondo, AIP Conf. Proc. **1085**, 727 (2009).
[18] X.-J. Bi, Y. Gao, J. Guo, N. Houston, T. Li, F. Xu, and X. Zhang, Phys. Rev. D **103**, 043018 (2021).
[19] V. Q. Tran, T. T. Q. Nguyen, and T.-C. Yuan, J. Cosmol. Astropart. Phys. 05 (2024) 015.
[20] S.-P. Li and X.-J. Xu, J. Cosmol. Astropart. Phys. 09 (2023) 009.
[21] D. Wadekar and G. R. Farrar, Phys. Rev. D **103**, 123028 (2021).
[22] M. J. Dolan, F. J. Hiskens, and R. R. Volkas, J. Cosmol. Astropart. Phys. 05 (2024) 099.
[23] S. Dubovsky and G. Hernández-Chifflet, J. Cosmol. Astropart. Phys. 12 (2015) 054.
[24] S. Yan, L. Li, and J. Fan, J. High Energy Phys. 06 (2024) 028.
[25] D. K. Hong, C. S. Shin, and S. Yun, Phys. Rev. D **103**, 123031 (2021).
[26] N. Vinyoles, A. Serenelli, F. L. Villante, S. Basu, J. Redondo, and J. Isern, J. Cosmol. Astropart. Phys. 10 (2015) 015.
[27] G. Bertone, D. Hooper, and J. Silk, Phys. Rep. **405**, 279 (2005).
[28] G. Bertone and D. Hooper, Rev. Mod. Phys. **90**, 045002 (2018).
[29] G. Bertone and T. M. P. Tait, Nature (London) **562**, 51 (2018).
[30] G. Servant and T. M. P. Tait, Nucl. Phys. **B650**, 391 (2003).
[31] L. D. Landau, Dokl. Akad. Nauk SSSR **60**, 207 (1948).
[32] C.-N. Yang, Phys. Rev. **77**, 242 (1950).
[33] M. Pospelov, A. Ritz, and M. B. Voloshin, Phys. Lett. B **662**, 53 (2008).
[34] T. T. Q. Nguyen and T. M. P. Tait, Phys. Rev. D **107**, 115016 (2023).
[35] T. T. Q. Nguyen, T. Linden, P. Carenza, and A. Widmark, arXiv:2501.14864.
[36] T. T. Q. Nguyen, in Windows on the Universe: 30th Anniversary of the Rencontres du Vietnam (2023), arXiv:2312.12292.
[37] S. D. McDermott, H. H. Patel, and H. Ramani, Phys. Rev. D **97**, 073005 (2018).
[38] H. Yuksel and M. D. Kistler, Phys. Rev. D **78**, 023502 (2008).
[39] T. Linden, T. T. Q. Nguyen, and T. M. P. Tait, arXiv:2402.01839.
[40] J. F. Navarro, C. S. Frenk, and S. D. M. White, Astrophys. J. **490**, 493 (1997).
[41] E. V. Karukes, M. Benito, F. Iocco, R. Trotta, and A. Geringer-Sameth, J. Cosmol. Astropart. Phys. 05 (2020) 033.
[42] J. Iguaz, J. Iguaz, P. D. Serpico, P. D. Serpico, T. Siegert, and T. Siegert, Phys. Rev. D **103**, 103025 (2021); **107**, 069902(E) (2023).
[43] R. Essig, E. Kuflik, S. D. McDermott, T. Volansky, and K. M. Zurek, J. High Energy Phys. 11 (2013) 193.
[44] R. Essig *et al.*, in Snowmass 2013: Snowmass on the Mississippi (2013), arXiv:1311.0029.
[45] J. R. Ellis, G. B. Gelmini, J. L. Lopez, D. V. Nanopoulos, and S. Sarkar, Nucl. Phys. **B373**, 399 (1992).
[46] F. Iocco, G. Mangano, G. Miele, O. Pisanti, and P. D. Serpico, Phys. Rep. **472**, 1 (2009).
[47] E. Holtmann, M. Kawasaki, K. Kohri, and T. Moroi, Phys. Rev. D **60**, 023506 (1999).
[48] M. Kawasaki, K. Kohri, and T. Moroi, Phys. Rev. D **63**, 103502 (2001).
[49] T. Siegert, R. Diehl, M. G. H. Krause, and J. Greiner, Astron. Astrophys. **579**, A124 (2015).
[50] T. Siegert, R. Diehl, G. Khachatryan, M. G. H. Krause, F. Guglielmetti, J. Greiner, A. W. Strong, and X. Zhang, Astron. Astrophys. **586**, A84 (2016).
[51] T. Siegert, R. Diehl, J. Greiner, M. G. H. Krause, A. M. Beloborodov, M. Cadolle Bel, F. Guglielmetti, J. Rodriguez, A. W. Strong, and X. Zhang, Nature (London) **531**, 341 (2016).
[52] T. Siegert, R. Diehl, A. C. Vincent, F. Guglielmetti, M. G. H. Krause, and C. Boehm, Astron. Astrophys. **595**, A25 (2016).
[53] T. Siegert, Astron. Astrophys. **632**, L1 (2019).
[54] T. Siegert, R. M. Crocker, O. Macias, F. H. Panther, F. Calore, D. Song, and S. Horiuchi, Mon. Not. R. Astron. Soc. **509**, L11 (2021).
[55] F. Calore, A. Dekker, P. D. Serpico, and T. Siegert, Mon. Not. R. Astron. Soc. **520**, 4167 (2023).
[56] P. De la Torre Luque, S. Balaji, P. Carenza, and L. Mastrototaro, Phys. Rev. D **111**, L061303 (2025).
[57] J. Berteaud, F. Calore, J. Iguaz, P. D. Serpico, and T. Siegert, Phys. Rev. D **106**, 023030 (2022).
[58] T. Siegert, F. Calore, and P. D. Serpico, Mon. Not. R. Astron. Soc. **528**, 3433 (2024).
[59] T. Siegert, C. Boehm, F. Calore, R. Diehl, M. G. H. Krause, P. D. Serpico, and A. C. Vincent, Mon. Not. R. Astron. Soc. **511**, 914 (2022).
[60] T. Siegert, R. Diehl, C. Weinberger, M. M. M. Pleintinger, J. Greiner, and X. Zhang, Astron. Astrophys. **626**, A73 (2019).
[61] R. Krivonos, M. Revnivtsev, E. Churazov, S. Sazonov, S. Grebenev, and R. Sunyaev, Astron. Astrophys. **463**, 957 (2007).
[62] W. Wang, T. Siegert, Z. G. Dai, R. Diehl, J. Greiner, A. Heger, M. Krause, M. Lang, M. M. M. Pleintinger, and X. L. Zhang, Astrophys. J. **889**, 169 (2020).
[63] T. Siegert, S. Ghosh, K. Mathur, E. Spraggon, and A. Yeddanapudi, Astron. Astrophys. **650**, A187 (2021).
[64] G. Vianello, R. J. Lauer, P. Younk, L. Tibaldo, J. M. Burgess, H. Ayala, P. Harding, M. Hui, N. Omodei, and H. Zhou (2015).
[65] D. Foreman-Mackey, D. W. Hogg, D. Lang, and J. Goodman, Publ. Astron. Soc. Pac. **125**, 306 (2013).
[66] H. An, M. Pospelov, and J. Pradler, Phys. Lett. B **725**, 190 (2013).
[67] E. Churazov *et al.*, Astron. Astrophys. **467**, 529 (2007).
[68] G. Weidenspointner, M. Varendorff, S. C. Kappadath, K. Bennett, H. Bloemen, R. Diehl, W. Hermsen, G. G. Lichti, J. Ryan, and V. Schönfelder, AIP Conf. Proc. **510**, 467 (2000).

[69] A. W. Strong, I. V. Moskalenko, and O. Reimer, Astrophys. J. **613**, 962 (2004).
[70] T. T. Q. Nguyen, I. John, T. Linden, and T. M. P. Tait, arXiv:2412.00180.
[71] T. T. Q. Nguyen, Proc. Sci. COSMICWISPers2024 (**2025**) 066.
[72] T. T. Q. Nguyen, P. De la Torre Luque, I. John, S. Balaji, P. Carenza, and T. Linden (to be published).
[73] C. O'Hare, cajohare/axionlimits: Axionlimits, https://cajohare.github.io/AxionLimits/URL (2020).
[74] D. Wouters and P. Brun, Astrophys. J. **772**, 44 (2013).
[75] M. C. D. Marsh, H. R. Russell, A. C. Fabian, B. P. McNamara, P. Nulsen, and C. S. Reynolds, J. Cosmol. Astropart. Phys. 12 (2017) 036.
[76] C. S. Reynolds, M. C. D. Marsh, H. R. Russell, A. C. Fabian, R. Smith, F. Tombesi, and S. Veilleux, Astrophys. J. **890**, 59 (2020).
[77] J. S. Reynés, J. H. Matthews, C. S. Reynolds, H. R. Russell, R. N. Smith, and M. C. D. Marsh, Mon. Not. R. Astron. Soc. **510**, 1264 (2021).
[78] J. W. Foster, M. Kongsore, C. Dessert, Y. Park, N. L. Rodd, K. Cranmer, and B. R. Safdi, Phys. Rev. Lett. **127**, 051101 (2021).
[79] P. De la Torre Luque, S. Balaji, and P. Carenza, Phys. Rev. D **109**, L101305 (2024).
[80] K. Perez, K. C. Y. Ng, J. F. Beacom, C. Hersh, S. Horiuchi, and R. Krivonos, Phys. Rev. D **95**, 123002 (2017).
[81] K. C. Y. Ng, B. M. Roach, K. Perez, J. F. Beacom, S. Horiuchi, R. Krivonos, and D. R. Wik, Phys. Rev. D **99**, 083005 (2019).
[82] B. M. Roach, S. Rossland, K. C. Y. Ng, K. Perez, J. F. Beacom, B. W. Grefenstette, S. Horiuchi, R. Krivonos, and D. R. Wik, Phys. Rev. D **107**, 023009 (2023).
[83] C. Fong, K. C. Y. Ng, and Q. Liu, arXiv:2401.16747.
[84] R. Janish and E. Pinetti, Phys. Rev. Lett. **134**, 071002 (2025).
[85] H. An, S. Ge, J. Liu, and Z. Lu, arXiv:2402.17140.
[86] S. Roy, C. Blanco, C. Dessert, A. Prabhu, and T. Temim, Phys. Rev. Lett. **134**, 071003 (2025).
[87] T. Bessho, Y. Ikeda, and W. Yin, Phys. Rev. D **106**, 095025 (2022).
[88] W. Yin *et al.*, Phys. Rev. Lett. **134**, 051004 (2025).
[89] E. Todarello, M. Regis, J. Reynoso-Cordova, M. Taoso, D. Vaz, J. Brinchmann, M. Steinmetz, and S. L. Zoutendijke, J. Cosmol. Astropart. Phys. 05 (2024) 043.
[90] C. Thorpe-Morgan, D. Malyshev, A. Santangelo, J. Jochum, B. Jäger, M. Sasaki, and S. Saeedi, Phys. Rev. D **102**, 123003 (2020).
[91] A. De Angelis *et al.*, Exp. Astron. **51**, 1225 (2021).
[92] C. Dessert, O. Ning, N. L. Rodd, and B. R. Safdi, Phys. Rev. Lett. **132**, 211002 (2024).
[93] D. Barret *et al.*, arXiv:1308.6784.
[94] J. Sisk-Reynés, C. S. Reynolds, M. L. Parker, J. H. Matthews, and M. C. D. Marsh, Astrophys. J. **951**, 5 (2023).
[95] J. W. D. Halliday *et al.*, Phys. Rev. Lett. **134**, 055001 (2025).
[96] C. R. Harris *et al.*, Nature (London) **585**, 357 (2020).
[97] P. Virtanen *et al.*, Nat. Methods **17**, 261 (2020).
[98] T. P. Robitaille *et al.* (ASTROPY Collaboration), Astron. Astrophys. **558**, A33 (2013).
[99] J. D. Hunter, Comput. Sci. Eng. **9**, 90 (2007).
[100] T. Kluyver, B. Ragan-Kelley, F. Pérez, B. Granger, M. Bussonnier, J. Frederic, K. Kelley, J. Hamrick, J. Grout, S. Corlay, P. Ivanov, D. Avila, S. Abdalla, and C. Willing (JUPYTER Development Team), in IOS Press (2016) pp. 87–90.
[101] D. Binosi, J. Collins, C. Kaufhold, and L. Theussl, Comput. Phys. Commun. **180**, 1709 (2009).
[102] A. Rohatgi, WEBPLOTDIGITIZER: Version 4.6 (2022).